Wintertime circulation off southeast Australia: Strong forcing by the East Australian Current

John F. Middleton
School of Mathematics, University of New South Wales, Sydney, New South Wales, Australia

Mauro Cirano
Centro de Pesquisa em Geofisica e Geologia, Universidade Federal da Bahia, Salvador, Brazil

Received 21 December 2004; revised 18 April 2005; accepted 22 September 2005; published 13 December 2005.

[1] Numerical results and observations are used to examine the sub–weather band wintertime circulation off the eastern shelf slope region between Tasmania and Cape Howe. The numerical model is forced using wintertime-averaged atmospheric fluxes of momentum, heat, and freshwater and using transports along open boundaries that are obtained from a global ocean model. The boundary to the north of Cape Howe has a prescribed transport of 17 Sv, which from available observations represents strong forcing by the East Australian Current (EAC). Nonetheless, the model results are in qualitative (and quantitative) agreement with several observational studies. In accord with observations, water within Bass Strait is found to be driven to the east and north with speeds of up to 30 cm s^{-1} off the southeast Victorian coast. The water is colder and denser than that found farther offshore, which is associated with the southward flowing (warm) EAC. In agreement with observations the density difference between the two water masses is about 0.6 kg m^{-3} and leads to a cascade of dense Bass Strait water to depths of 300 m and as a plume that extends 5–10 km in the cross-shelf direction. Typical vertical velocities of the model cascade are 20 m d^{-1}. Along-isobath currents become bottom intensified with speeds of 20 cm s^{-1} or so at depths of 200 m. The EAC is found to flow along isobaths and to the south and then west past Tasmania with speeds of up to 20 cm s^{-1}. Mesoscale eddies grow to diameters of 100 km (speeds <40 cm s^{-1}), and in accord with observations a semipermanent anticyclonic eddy is found to the east of Cape Howe.

Citation: Middleton, J. F., and M. Cirano (2005), Wintertime circulation off southeast Australia: Strong forcing by the East Australian Current, *J. Geophys. Res.*, *110*, C12012, doi:10.1029/2004JC002855.

1. Introduction

[2] There have been relatively few studies of the sub—weather band wintertime coastal and oceanic circulation off southeast Australia: the region here is taken as the east coast of Tasmania, the eastern region of Bass Strait, Cape Howe and the adjacent Tasman Sea (Figure 1). Using current meter data, *Baines et al.* [1991] estimated the time-averaged eastward transport of water through the Bass Strait during winter to be 0.5 Sv. Other data from the northeastern corner of the strait [*Godfrey et al.*, 1980; *Tomczak*, 1985; *Black et al.*, 1992] indicate mean alongshore currents of around 20 cm s^{-1} that are directed along slope, to the east and northeast and in water depths ranging from 50 to 370 m. During winter, water within the strait is driven to the north near Cape Howe.

[3] Indeed, the fate of the Bass Strait water is related to the Bass Strait "cascade" whereby wintertime cooling of the saline waters within the strait leads to the formation of water that is denser than the adjacent water of the Tasman Sea. Water cascades to depths of 300 m or more and largely along the zonal shelf slope that defines the northeast corner of Bass Strait and the Cape Howe region [*Godfrey et al.*, 1980; *Tomczak*, 1985; *Luick et al.*, 1994]. For the same density, the strait water is more saline and warmer than the adjacent Tasman Seawater and appears as a warm, saline anomaly in hydrographic data collected as far north as Jervis Bay (35°S).

[4] The northern extent and location of the Bass Strait water does seem to be dependent on the strength of the East Australian Current (EAC) and the presence or not of mesoscale eddies near the Cape Howe region. The EAC is somewhat seasonal and hydrographically derived estimates of its southward transport at 28°S indicate summer and winter maxima of 36 Sv and 27 Sv respectively [*Ridgway and Godfrey*, 1997]: a 2000 db level of no-motion was assumed. More recently, current meter observations have indicated that the transport near 30°S to be highly variable with flow reversals of more than 20 Sv over periods of 50 to 170 days [*Mata et al.*, 2000]. We have also used the hydrographic data contained in the CSIRO Atlas of Regional Seas (CARS) [*Ridgway et al.*, 2002] to determine

0148-0227/05/2004JC002855

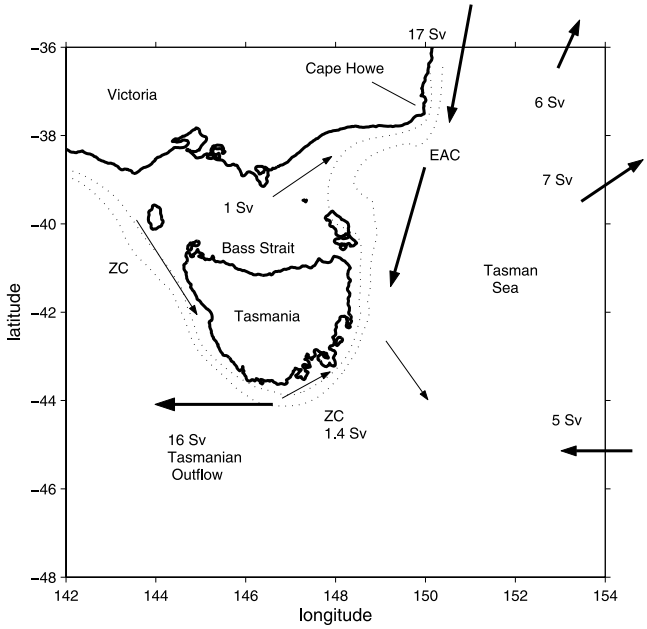

Figure 1. The domain of interest featuring Bass Strait and the Tasman Sea. The dotted lines denote the 200 and 1000 m isobaths where depth increases away from the coast. The major current systems including the Zeehan Current (ZC) and East Australian Current (EAC) are labeled and the associated transports are given (in Sverdrups) [see also *Cirano and Middleton*, 2004]. As shown, the EAC deflects the Zeehan Current offshore of the east Tasmanian coast. The transports along the eastern boundary are described in the text.

transports off Cape Howe (37°S). Assuming a 2000 db level of no motion, we obtain transports of 12 Sv for both summer and winter and for the zonal section 150°–152°E.

[5] The transports at Cape Howe and Bass Strait outflow, will also be strongly affected by mesoscale eddies. A decade long sequence of sea surface temperature (SST) images and surface velocity has been determined for the region using TOPEX/ERS altimetric and other remotely sensed data [*Griffin et al.*, 2002]. The wintertime data (Figure 2 (top)) shows currents near the slope of Cape Howe are generally directed to the south and form part of a (200 km diameter) mesoscale anticyclonic eddy. The warm core eddy is found here during 7 out of the 10 August periods (winters) between 1990 and 1999 and little cold Bass Strait water is found at the surface and far to the north of Cape Howe. The northward movement of cold Bass Strait water is either hindered by the southward currents of the anticyclonic eddy, or largely downwelled as suggested by *Luick et al.* [1994]. Their hydrographic survey (July 1989) was conducted during a period of strong southward excursion of the EAC and when an anticyclonic eddy was present off Cape Howe.

[6] During 1990, 1995 and 1996, the wintertime SST and circulation patterns were quite different and typified by that illustrated in Figure 2 (bottom). The flow is to the north near Cape Howe and the equatorward, coastal surface outflow expected from Bass Strait should no longer be retarded. Indeed, cold surface water is found far to the north of Cape Howe as shown in Figure 2 (bottom).

[7] An outline of the likely circulation to the south and east of Tasmania has been given by *Cresswell* [2000]. Drifters were found to track the coastal Zeehan Current from the west to the east Tasmanian coast. Between 43° and 41.5°S, these drifters and the coastal current were found to converge with the southward EAC and be swept away from the shelf and to the south. Off the southern tip of Tasmania, 6 hydrographic sections were also used to infer the existence of a westward "Tasmanian Outflow" [*Rintoul and Sokolov*, 2001]. The associated mean westward transport was found to be 8 Sv, highly variable (−5 to 21 Sv) and related to the latitude of the zero of wind stress curl that separates the anticyclonic subtropical gyre and cyclonic subpolar gyre. Where the zero line occurs well south of Tasmania, the EAC flows farther south and the Tasman Outflow is larger.

[8] The picture of the wintertime circulation above is determined from a handful of studies made over the last 20 years or so. The purpose of this note is to reexamine these and other observations, in the context of results from a numerical circulation model of the region. The model is that used by *Cirano and Middleton* [2004] where the primary aim was to study the circulation between South Australia and west Tasmania as forced by wintertime-averaged winds and surface fluxes. Thus the results here contain no information regarding the weather band [e.g., *Middleton and Black*, 1994] or tidal circulation [e.g., *Fandry*, 1983].

[9] The model topography, hydrography and forcing fields are only approximately representative of conditions of the region. In particular, the southward EAC transport used to drive the northern boundary within 200 km of Cape Howe is 17 Sv and 50% larger than the mean (12 Sv) noted above: both estimates are for the inshore branch of the EAC. However, the real transport of the region may well reach 17 Sv because of several factors. As noted above, changes in transport of 20 Sv can arise from eddy variability [*Mata et al.*, 2000]. The observations of *Luick et al.* [1994] also support the existence of strong southward excursions by the EAC. Second, the observed variability of the Tasman Outflow found by *Rintoul and Sokolov* [2001] is large and westward values of up to 21 Sv are obtained when the subtropical wind gyre extends farther south. From the model results below, it seems likely that the variability and strength of the outflow is proportional to that of the EAC near Cape Howe. Finally, a third factor that may enhance the transport of the EAC involves La Nina events. The results of *Wijffels and Meyers* [2004] show that positive (negative) sea level anomalies are found off Cape Howe and are correlated with westward (eastward) wind stress anomalies near the equator. Within 200 km of the coast, these anomalies are up to 6 cm in magnitude and the associated southward geostrophic velocity about one third of the current associated with the mean field dynamic height [*Ridgway and Godfrey*, 1997] (Figure 4). That is, during La Nina events, the transports of the EAC may be one third larger (4 Sv) than the 12 Sv estimated from the dynamic height field. In any case we will see that the model results do reproduce many of the observed circulation features.

2. Model

[10] A high-resolution version of the Princeton Ocean Model [*Blumberg and Mellor*, 1987] was adapted for the

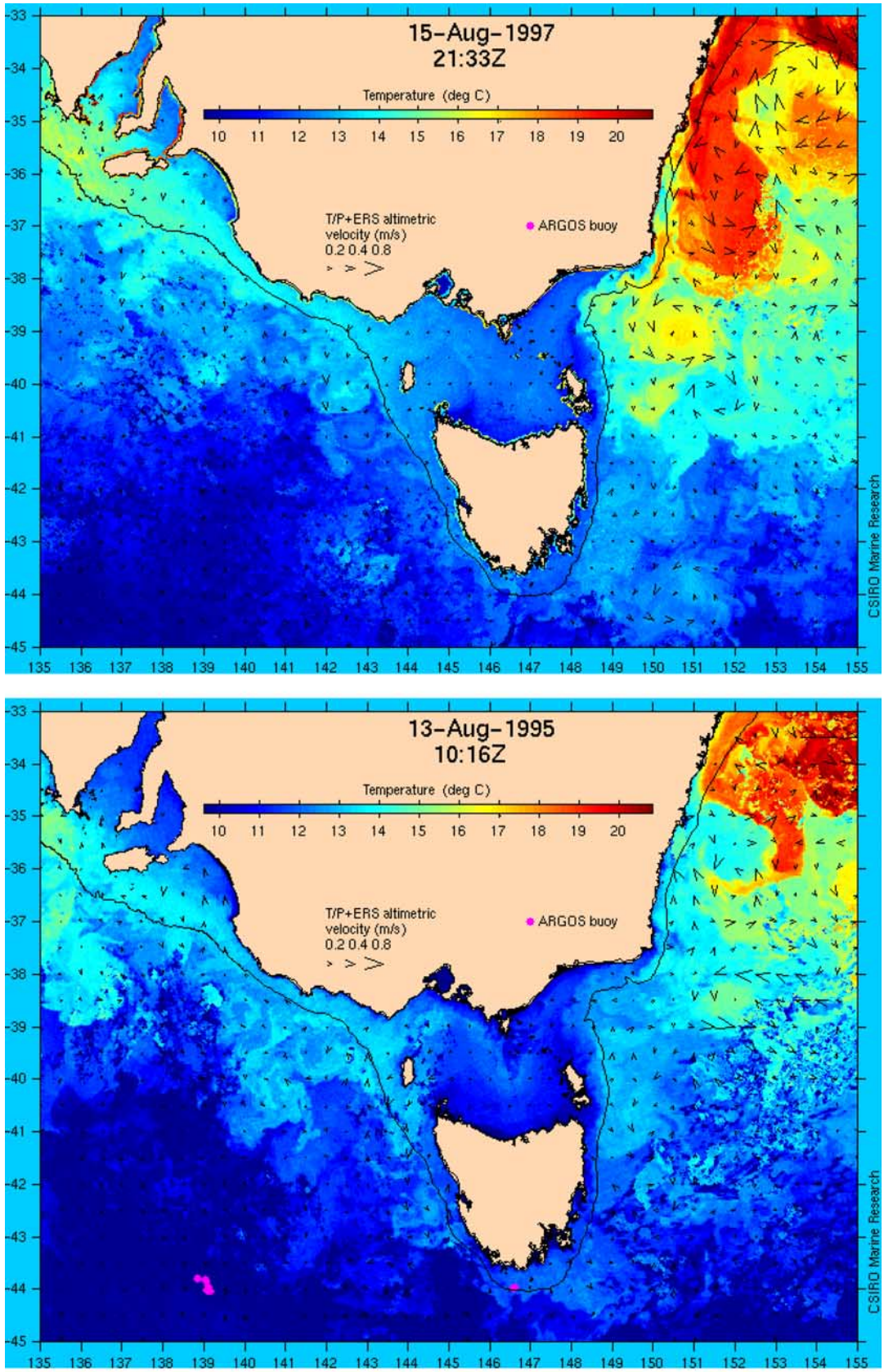

Figure 2. Sea surface temperature and surface currents (the arrowheads) inferred from TOPEX/ERS altimetric sea level data using geostrophy for (top) 15 August 1997 and (bottom) 13 August 1995. The 200 m isobath is indicated. (©CSIRO Marine and Atmospheric Research, reproduced with permission from *Griffin et al.*, [2002].)

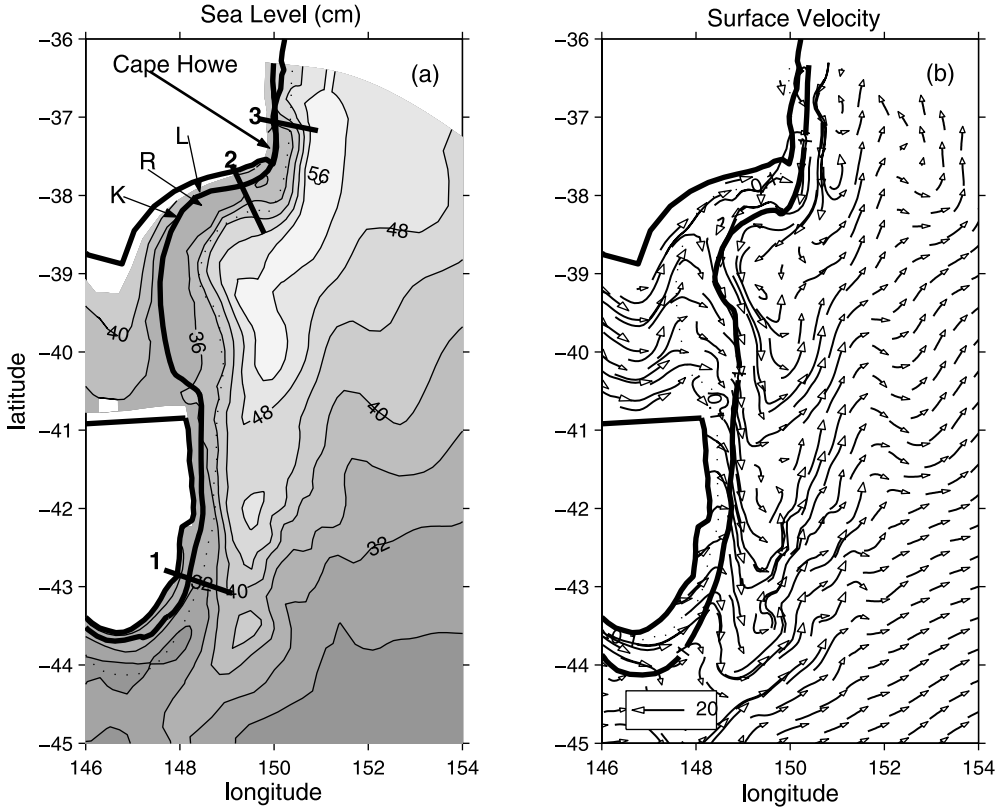

Figure 3. (a) The sea level field at day 56 (contour interval 4 cm) and for the region of interest. The locations of the transects off Maria Island (transect 1), Lakes Entrance (transect 2) and Cape Howe (transect 3) are indicated. Also indicated by arrows are the approximate locations of the current meter sites L (3 sites), K (1 site) and R (1 site) in Bass Strait. The solid and dotted curves correspond to the 100 and 1000 m isobaths. The coastline topography is that adopted in the model. The location of the northern open boundary is indicated by the unshaded region. (b) As in Figure 3a but for the surface velocity field at day 56. A vector of magnitude 20 cm s^{-1} is indicated. Note, the solid and dotted curves now indicate the 1000 and 100 m isobaths.

region [*Cirano and Middleton*, 2004] (hereinafter referred to as CM), with an alongshore resolution of 10–20 km and cross-shore resolution of 2–7 km. Thirty-two sigma levels in the vertical were assumed. The Mellor-Yamada turbulence closure scheme is adopted in the vertical, along with a quadratic bottom stress and constant horizontal diffusivity (100 m^2 s^{-1}).

[11] Forcing along the open boundaries was accomplished by relaxation to the wintertime depth-averaged transports of the global $^1/_4$ degree OCCAM model [*Webb et al.*, 1998; *Webb*, 2000]. For the open boundary to the north of Cape Howe, the OCCAM transport within 200 km of the coast is 17 Sv to the south and will act to block any northward outflow from Bass Strait.

[12] The surface was forced using an August-averaged wind stress field [*Trenberth et al.*, 1989] that is directed to the east for the subdomain of interest here (Figure 3) and with a magnitude of about 0.07 Pa (see CM). The associated Ekman transport is directed to the north and will only influence the circulation within Bass Strait where it is blocked by the Victorian and Tasmanian coasts (see below).

[13] Surface fluxes of heat and freshwater were also applied in determining the results here using an August-averaged climatology [*da Silva et al.*, 1994]. For the domain here, the net heat loss (Q) increases from 50 Wm^{-2} within Bass Strait to 100 Wm^{-2} off Cape Howe reflecting the increased sea surface temperature of the EAC. The net evaporation less precipitation flux (E) is negative within Bass Strait (-1×10^{-3} m d^{-1}) indicating a freshening of waters while to the east of the strait it is smaller and positive ($<0.05 \times 10^{-3}$ m d^{-1}). Oceanic fluxes of heat and salt are notoriously unreliable. However, we may examine their expected influence by considering their effect on the temperature T and salinity S, for a column of well-mixed water, depth H, and where advection is ignored. Following *Gill* [1982], the change in temperature (ΔT) and salinity (ΔS) over a time t due to the above fluxes are $\Delta T = -Qt/(\rho CH)$ and $\Delta S/S(0) = \Delta H/H$, where $\rho = 1025$ and $C = 4000$ J/(kg °K) are the density and heat capacity of seawater, S(0) is an initial salinity and $\Delta H = Et$ is the change in water column height due to the freshwater flux E. For Bass Strait the surface mixed layer extends to the seafloor and a scale for H is 50 m. For the wintertime Tasman Sea, the surface mixed layer H is around 150 m (see below).

[14] Now for salinity, the freshwater flux E is so small that the salinity will change by less than 0.1% over a period of 50 days and for both Bass Strait and the Tasman Sea. For temperature, the above fluxes over 50 days should lead to 1°

drop in temperature within Bass Strait (we find 1.5° below) and 0.2° for the Tasman Sea: the latter will prove small compared to warming due to advection by the EAC.

[15] With the exception of Bass Strait, the density fields are thus not sensitive to these (poorly known) fluxes and will depend rather on the initial values of T and S that we have taken from the wintertime OCCAM model. One advantage to using the OCCAM T/S fields is that they are dynamically adjusted to the applied forcing and larger-scale circulation of the OCCAM model. Since the forcing and large-scale circulation here are similar to OCCAM, the spin-up time for our model is of order 40–50 days (and not years): see below. A downside is that errors in the OCCAM near-surface fields in OCCAM (which are relaxed to Levitus) will appear in our higher-resolution model. We discuss this further below.

[16] The sea level and velocity fields are all initially zero and the model circulation spins-up over a period of 40–50 days. Indeed, in the absence of surface fluxes of heat and freshwater, CM find the volume-averaged kinetic energy and details of the circulation to change little between 50 and 90 days. The similarity of their large-scale results with those here indicates that the model results below are also in a quasi-steady state. Presentation of results for periods longer than 50–60 days also does not seem warranted. The surface and boundary forcing applied here are steady but in reality change on seasonal (90 day) timescale. In addition, with the strong forcing by the EAC, the results presented at day 56 of model integration replicate many of the observations.

3. Results

[17] Here we first examine the large-scale and surface fields for T, S and density. We show that while the model waters are warmer and fresher than observations, a front is found between the waters of Bass Strait and the Tasman Sea and with a density difference and scale that is in accord with observations. The model cascade found should therefore provide a first-order description of that found in reality. We then compare the model results with CTD, current meter and drifter data for 3 transects off Maria Island (Tasmania), northeast Bass Strait (the cascade) and Cape Howe. Reasonable agreement is found in each case and new information about the cascade determined.

3.1. Large-Scale Results and Sea Surface Fields

[18] The model sea level and surface velocity fields at day 56 are shown in Figure 3. Within 200 km of the northern boundary, the 17 Sv inflow leads to an EAC that flows to the south and principally seaward of the 1000 m isobath (Figure 3b). The net transports into the model are also illustrated in Figure 1. The return leg of the EAC carries about 6 Sv back to the north-northeast between 200 and 400 km from the coast. Farther to the east and along the open boundary, an additional 7 Sv is also directed to the northeast. South of 43°S, a general westward drift of 5 Sv occurs. The transports in and out of the eastern model domain are smaller compared to that which enters off Cape Howe. Indeed, the surface and depth-averaged results do indicate that most of the 17 Sv that enters the model off Cape Howe flows to the south and then west past the southern tip of Tasmania. Indeed, part of the southward

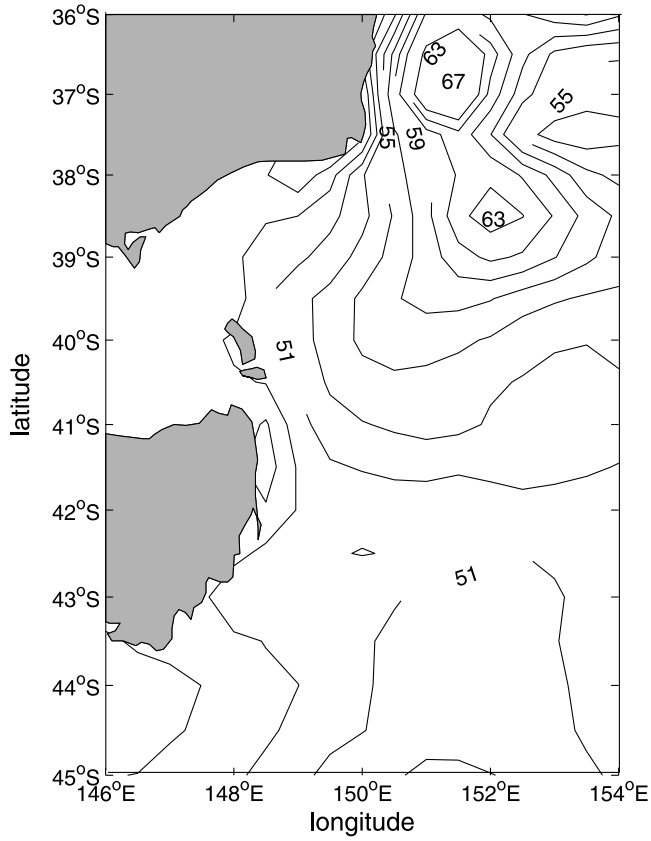

Figure 4. The winter-averaged (July–September) dynamic height (centimeters) relative to the 2000 db level as obtained from the CARS climatology.

flow becomes intensified with depth and at the 146°E meridional section, (south of Tasmania), is manifest as a westward current (the Tasman Outflow) with a maximum speed of 20 cm s^{-1} at a depth of 800 m (CM, Figure 17). The westward model transport within 200 km of the coast is 16 Sv. The value is close to that specified on the northern boundary of Cape Howe. The 16 Sv is twice the mean found by *Rintoul and Sokolov* [2001], but again within their annual estimate of (−5, 21) Sv. The model density structure is also very similar to that obtained from these hydrographic sections [*Rintoul and Bullister*, 1999], with a 400 m deep surface mixed layer, downwelling to depths of 400 m near the shelf and upwelling between 1500 m and 800 m over the slope (CM).

[19] The results in Figure 3 also show that the EAC has broken up into several anticyclonic eddies with diameters of 100 to 200 km. The radial speeds of the eddies immediately east of Bass Strait and Cape Howe (Figure 3b) are of order 20 cm s^{-1} and about one half of that inferred from the "snapshots" of altimeter and SST data in Figure 2 (top).

[20] The anticyclonic eddies to the east of Cape Howe and the strait are also found in the winter climatology of dynamic height relative to 2000 db (Figure 4) that has been obtained from the CSIRO Atlas of Regional Seas (CARS) [*Ridgway et al.*, 2002]. The difference in dynamic height between the high off Cape Howe and the northeast tip of Tasmania is about 23 cm and comparable to the 20 cm difference found in the model results (Figure 3a).

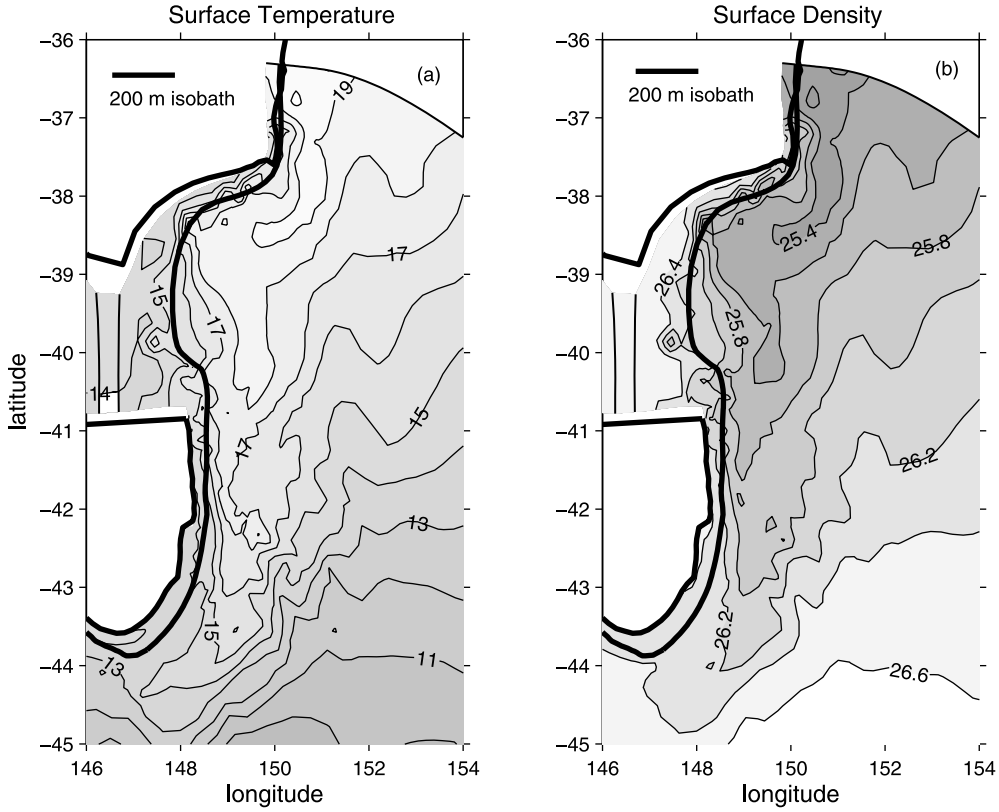

Figure 5. (a) The sea surface temperature field at day 56 (contour interval 1°). (b) The sea surface density field at day 56 (interval 0.2 kg m^{-3}). The solid line indicates the 200 m isobath.

[21] We now compare the model T, S and density surface fields with observations. First consider the northeast region of Bass Strait. Here, the model temperature drops from about 15.5° at day 0 to 14.5° at day 56 (Figure 5a). This result is in agreement with that expected for atmospheric cooling (see Section 2). The temperature of 14.5° is slightly larger than that indicated by CARS (∼13.5°) and the wintertime hydrographic data obtained by *Luick et al.* [1994] where T ∼ 14°. The model salinity here is 35.4 ppt and unchanged from day zero since the freshwater fluxes are negligible. The model salinity is however 0.1 ppt less than that indicated by the CARS climatology and survey results of *Luick et al.* [1994], where water of 35.5 ppt typically has a temperature of 14° and density of about 26.6–26.7 kg m^{-3}. Indeed, the slightly warmer, fresher water leads to a model density at the northeast corner of the strait that is about 26.4 kg m^{-3} (Figure 5b) and about 0.2 kg m^{-3} lighter than that of CARS or *Luick et al.* [1994].

[22] Now consider the surface properties of the Tasman Sea to the immediate east of Bass Strait and near the region of the expected cascade (38.5°S, 149°E). The model surface temperature from Figure 5a is about 18° and 2° warmer than at day 0. In addition, the model water is also 2° warmer that indicated by the satellite image in Figure 2 (top) and by the CARS data. The surface cooling adopted should have led to a 0.2° drop in temperature. The 2° increase is due to the southward advection of warm 19° water by the model EAC, where over 50 days or so, the 10–20 cm s^{-1} currents will move water 350 km or more to the south. The model salinities within the Tasman Sea are about 35.3 ppt and 0.1–0.2 ppt fresher than CARS or the results of *Luick et al.* [1994]. The resultant model density at the surface and near (38.5°S, 149°E) is about 25.6 kg m^{-3} and again 0.2 kg m^{-3} smaller than that indicated by the observations. However, the width of the front and density difference (0.6–0.8 kg m^{-3}) between Bass Strait and the Tasman Sea are both in good agreement with the transect data of *Luick et al.* [1994]. Results for the cascade below should therefore be applicable to the real ocean.

3.2. Near-Slope Circulation and Vertical Structure off Tasmania

[23] Off the east coast of Tasmania, the model results (Figure 3b) indicate an equatorward coastal current of up to 20 cm s^{-1}. This current is an extension of the Zeehan Current that flows southward down the west Tasmanian coast and then enters the domain near 146°E as an eastward coastal current (maximum speed 20 cm s^{-1}) that extends to depths of 500 m and with a transport of about 1 Sv (CM). The Zeehan Current reproduced by the model is in reasonable agreement with observations obtained on the west coast of Tasmania (CM). As noted, evidence for its continuation along the east coast comes from surface drifters of *Cresswell* [2000]. From Figure 3a, the model results also indicate this extension of the Zeehan Current to converge with the southward flowing EAC whereby water is swept offshore between 43°S and 41.5°S: near 41.5°S, the model coastal current is near zero or has reversed. This picture is in agreement with that inferred by *Cresswell* [2000] from drifter data.

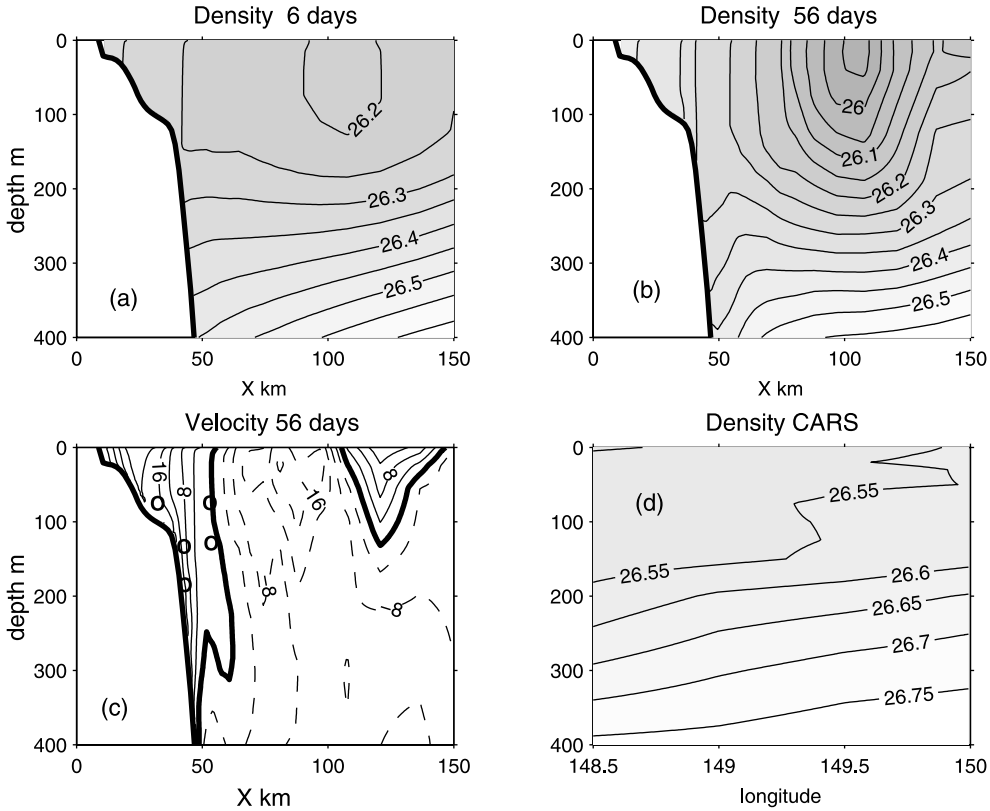

Figure 6. Results for the zonal transect 1 (J = 128) off Maria Island (42.9°S): (a) the model density field at day 6 (interval 0.05 kg m^{-3}), (b) the model density field at day 56 (interval 0.05 kg m^{-3}), and (c) the along-isobath velocities (contour interval 4 cm s^{-1}). Solid contours indicate flow to the north. The circles denote the locations of the Maria Island current meters (Table 1). (d) The CARS wintertime-averaged density field at 42.5°S and for the approximate location of transect 1 (interval 0.05 kg m^{-3}).

[24] Results for three cross-shelf transects (noted in Figure 3a) were also obtained and those for the Tasmanian region are shown in Figure 6. The advection of warm light water into this region is illustrated by the core of relatively light water in the top 300 m from day 0 (Figure 6a) to day 56 (Figure 6b). The maximum southward speed of the EAC is 18 cm s^{-1} (Figure 6c). The CARS wintertime data (Figure 6d) indicate that denser water should found here (~26.5–26.7 kg m^{-3}). While no EAC light core of water is apparent in the CARS data (Figure 6d), encouragingly, both this data and model field at day 56 do indicate that water is well mixed vertically to depths of 150–200 m.

[25] Figure 6c also shows the approximate shelf and slope sites of current meters deployed in 1983 as part of the Australian Coastal Experiment [e.g., *Huyer et al.*, 1988] and in 1988 by the CSIRO. (Further details of this and other data are listed in the caption of Table 1.) Only data up until the end of November was used so as to obtain austral "wintertime" average statistics. These were determined by low-pass filtering the data [*Thompson*, 1983] and then resolving the currents along the major and minor axes. The directions of the major axes in all cases are to the north or north-northeast, along the shelf and the mean currents range from 2–10 cm s^{-1} near the coast, to 20 cm s^{-1} farther offshore and over the 1000 m isobath. The model results (Figure 6c) suggest stronger equatorward flow near the coast and weaker (even poleward) flow offshore. The observed 20 cm s^{-1} northward flow over the 1000 m isobath is not reproduced. In this context, we note that the RMS variability for this and other meter sites is comparable to the mean (Table 1) and the offshore currents can be influenced by mesoscale eddies (Figure 2 (top)). Qualitative support for the model currents is given however by a December ADCP transect [*Cresswell*, 2000] made farther north (41.7°S) with northward shelf currents (up to 20 cm s^{-1}) and southward currents farther offshore (up to 40 cm s^{-1}).

3.3. Near-Slope Circulation: Bass Strait

[26] For the northeast region of Bass Strait, an eastward current of up to 20 cm s^{-1} is found near the 100 m isobath (Figure 3b). The eastward transport through the strait is 0.95 Sv (CM). For quasi-steady motion, the transport U through the strait is subject to geostrophic control [*Garrett and Toulany*, 1982; CM] and fixed by the sea level difference $\Delta\eta$ across the eastern strait mouth

$$U = -gH\Delta\eta/f \quad (1)$$

where g denotes the acceleration by gravity, H the water depth and *F* the Coriolis parameter. For Bass Strait, $\Delta\eta$ and U can be effected by the transport entering the western mouth of the strait and sea level variations at the eastern mouth that may arise from the EAC and cascade of dense strait water into the Tasman Sea. An additional mechanism

Table 1. The EC 1988 (CSIRO) and Line 0 and Line 1 (the Australian Coastal Experiment [e.g., *Huyer et al.*, 1988]) Data Were Obtained From the CSIRO and the Statistics Below Determined[a]

I.D.	Latitude	Longitude	Instrument Depth, m	Water Depth, m	Start Time, d/mo	Length, days	V, σ_V	U, σ_U	°T
				1 Maria Islandland					
EC 1988	42.6507	148.2833	70	100	31/4	159	10.2 16.3	0.1 3.8	10
Line0 1983	42.6683	148.4517	125	200	1/10	60	2.5 11.4	−2.8 4.1	18
Line0 1983	42.6683	148.4517	190	200	1/10	60	6.0 6.9	3.0 4.1	46
EC 1988	42.6707	148.4703	71	1000	31/4	169	8.5 13.6	−0.1 4.3	−2
EC 1988	42.6707	148.4703	125	1000	31/4	169	20.6 26.8	−0.2 5.0	25
EC 1988	42.6707	148.4703	985	1000	31/4	157	2.2 1.8	0.1 1.0	46
				2 Bass Strait					
L 1990	37.9	148.25	10	20	1/6	41	11		∼90
L 1990			10	40	1/6	41	16		∼90
L 1990			10	50	1/6	41	21		∼90
K 1981	38.6000	148.1833	10	80	10/6	26	∼22		∼70
R 1975	38.55	148.55	350	370	7/7	18	∼20		0
				3 Cape Howe					
Line1 1983	37.5400	150.1833	125	140	11/9	75	9.9 23.8	0.7 4.5	37
Line1 1983	37.5417	150.2400	75	201	11/9	75	−3.2 20.9	0.0 6.9	23
Line1 1983	37.5417	150.2967	125	500	18/10	43	5.4 14.1	−1.6 5.2	17
Line1 1983	37.5417	150.2967	190	500	12/9	75	4.1 13.2	−1.4 3.9	24
Line1 1983	37.5417	150.2967	450	500	12/9	75	8.9 12.5	−0.4 1.7	16

[a]Only data up until the end of November were used so as to obtain "wintertime" statistics. All data were low-pass filtered, and the mean current speeds in the major (V) and minus (U) axis directions were determined along with the standard deviation (σ_V, σ_U) (Units cm s^{-1}). The direction of the major axis (°T: degrees clockwise from north) was determined as that direction with the largest standard deviation. For the sites at L the mean speeds come from *Black et al.* [1992] and the direction (east) is estimated. For site K (Kingfish-B) the mean was estimated from the progressive vector diagram given by *Tomczak* [1985]. For site R the mean was estimated from a plot given by *Godfrey et al.* [1980]. For each transect the results are ordered in terms of increasing water depth.

is the sea level difference that arises from zonal winds within the strait. Indeed, a simple model for the steady circulation driven by a zonal wind stress τ^W within the strait (CM) yields a net transport of

$$U_W = -\tau^W L/(f\rho) \quad (2)$$

or 0.3 Sv, where the length of the strait L is taken as 400 km and the wintertime average is that used in the model here; τ^W = 0.07 Pa. Thus, of the 0.95 Sv obtained from the numerical model, 30% arises from local wind forcing. The remainder will arise from the factors noted above.

[27] Current observations have been obtained at five sites near the northeast corner of the strait and their approximate locations, in order of increasing water depth (Table 1) are indicated by the symbols L (3 sites), K (1 site) and R (1 site) in Figure 3a. The estimates of the mean along-isobath currents at these sites (Table 1) within the strait are typically 10–20 cm s^{-1} and comparable with the model values that range up to 30 cm s^{-1} (Figure 3b).

[28] A more detailed investigation may be made by examination of the cross-shelf numerical results for the region (transect 2) that are presented in Figure 7: the density and current results are typical for the northeast corner of the strait. The equatorward alongshore velocity field here extends to more than 500 m with amplitudes of 15–30 cm s^{-1} over the slope and shelf (Figure 7c). The currents are also intensified with depth. For example, at the 200 m isobath, the alongshore current is about 16 cm s^{-1} and decreases with height to be near zero at the surface.

[29] The bottom intensification results from the thermal wind shear associated with the cascade and is supported by observations cited next. As shown in Figure 7a, strait water of density 26.3 kg m^{-3} cascades over the slope and to depths of 300 m or so. The plume width is of order 10 km. The associated vertical velocities are also shown in Figure 7d and can exceed 60 m d^{-1}. A hydrographic transect obtained a little farther to the east by *Tomczak* [1985], shows a similar phenomena (Figure 7b) although the plume width of 5 km is smaller. In either case, the thermal wind shear associated with the upward tilting density field of cascade water will lead to the bottom intensification of the along-slope velocities as illustrated by Figure 7c. Currents measured near this transect at site R by *Godfrey et al.* [1980] exhibit an along-isobath average flow of ∼20 cm s^{-1} at a depth of 350 m and 20 m from the bottom (Table 1). A single snapshot of current with height presented by these authors also shows the current to decrease in magnitude and then reverse direction in a manner that is qualitatively consistent with that shown in Figure 7c.

[30] The bottom boundary layer of these along-isobath currents is also downwelling favourable, although near the slope the shape of the density contours suggest dominance by the gravitational cascade. For the cascade, the level density contours offshore, slope up next to the shelf (Figure 7a). In the absence of a gravitational cascade, boundary layer mixing and downwelling would imply that the level density contours offshore slope down near the shelf [e.g., *Middleton and Ramsden*, 1996]. This is not found. Moreover, the plot (Figure 8a) of the vertical velocity at the bottom (day 56) indicates the cascade to be largest to the northeast of 38.5°S. Along this part of the shelf, the alongshore currents are largest, the shelf narrows and the density front is narrowest (Figure 5b). Cascade velocities

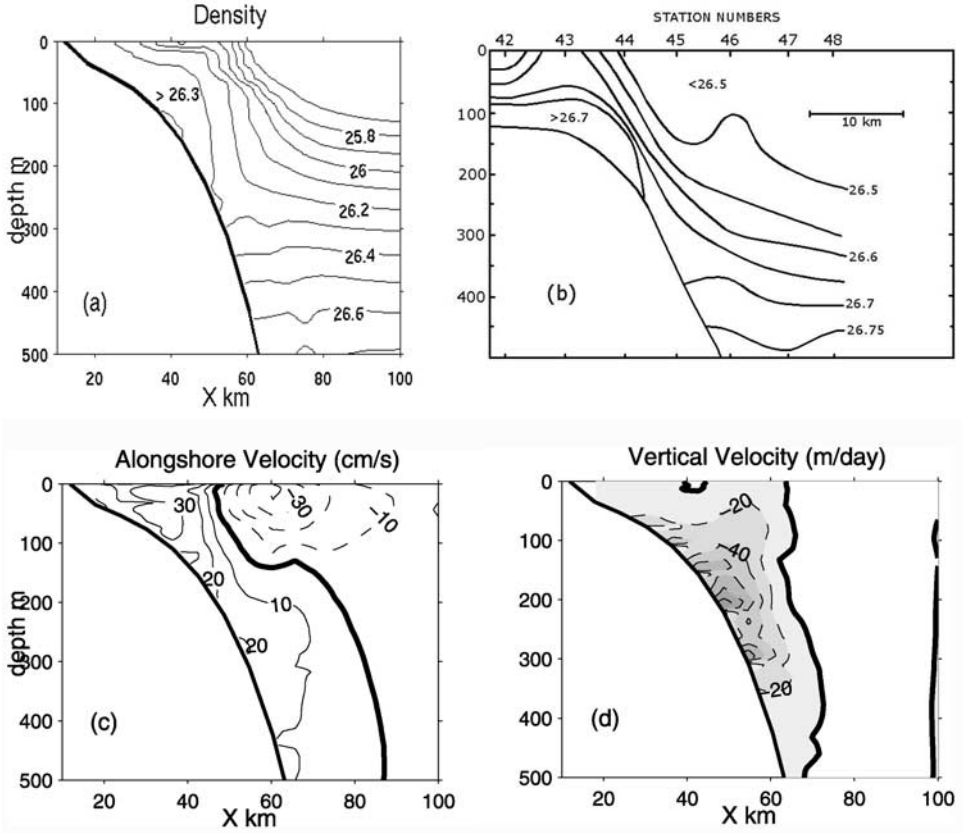

Figure 7. Results for the meridional transect 2 (J = 161) near Lakes Entrance (148.9°E). (a) The model density field at day 56 (interval 0.1 kg m^{-3}). (b) The density field measured by *Tomczak* [1985] close to the meridional transect in Figure 7a. The interval here is 0.05 kg m^{-3}. Results for the meridional transect 2 near Lakes Entrance (148.9°E). (c) The along-isobath velocities (contour interval 10 cm s^{-1}). Solid contours indicate flow to the east. (d) The vertical velocity (contour interval 20 m d^{-1}). Dashed (shaded) contours indicate downward flow.

of up to 120 m d^{-1} are found. Significantly, on the basis of CTD surveys both *Luick et al.* [1994] and *Tomczak* [1985] also concluded that the cascade was strongest in this region.

[31] Another feature apparent in Figure 8a is the strong upwelling (30–120 m d^{-1}) that occurs in very deep water (1000–2000 m) to the south of the main cascade region, and on the shoreward side of a large canyon. Results (not shown) indicate that the upwelling increases with time. The mechanism for upwelling is most likely that found for other canyons [e.g., *Klink*, 1996] and results from the shoreward acceleration by the cross-shelf pressure gradient. Scale estimates show the upwelling rate of 30 m d^{-1} can be driven by an ageostrophic flow across isobaths of 10^{-3} cm s^{-1}, or less than 0.01% of the typical alongshore currents for the region. (An across-isobath velocity of order 3 cm s^{-1} is shown in Figure 8b.) Thus only 0.01% of the (normally balanced) onshore pressure gradient is needed to drive the deep upwelling. The deep upwelling is of interest, but since we have no data to support its existence, little more will be said.

3.4. Near-Slope Circulation: Cape Howe

[32] Results for the Cape Howe line (transect 3) are shown in Figure 9. As indicated by the 26.1 kg m^{-3} density contour, the cascade is now reduced to a depth of 150 m. The equatorward coastal current is weaker (<20 cm s^{-1}) than within Bass Strait, presumably because of the convergence with the southward EAC (Figure 3b). The alongshore model results may be also be compared to the mean currents estimated from current meter data obtained for the Cape Howe region and from CSIRO (Table 1). The sites of the current meters is indicated in Figure 9b, and the estimates indicate an equatorward, mean flow of 4–10 cm s^{-1} that is generally weaker than obtained from the model (typically 15 cm s^{-1}). A weak southward flow for the meter moored at a depth of 75 m is also found while from Figure 9b the model current is 12 cm s^{-1} and to the north.

[33] The results for density (Figure 9a) also indicate isopycnals to be generally upwelled. Such upwelling is associated with the EAC itself and in this case, is intensified by the presence of the anticyclonic eddy off Cape Howe. Near the shelf slope, and at depths of more than 150 m, a downwelled bottom boundary layer is evident. The vertical velocity associated with the downwelling here is from Figure 8a about −30 m d^{-1}. The downwelled boundary layer is driven in part by bottom stress associated with the equatorward shelf slope currents. To show this, we first note that the vertical velocity may be estimated from the kinematic condition at the bottom $w_b = -u_b h_x$ with the shelf

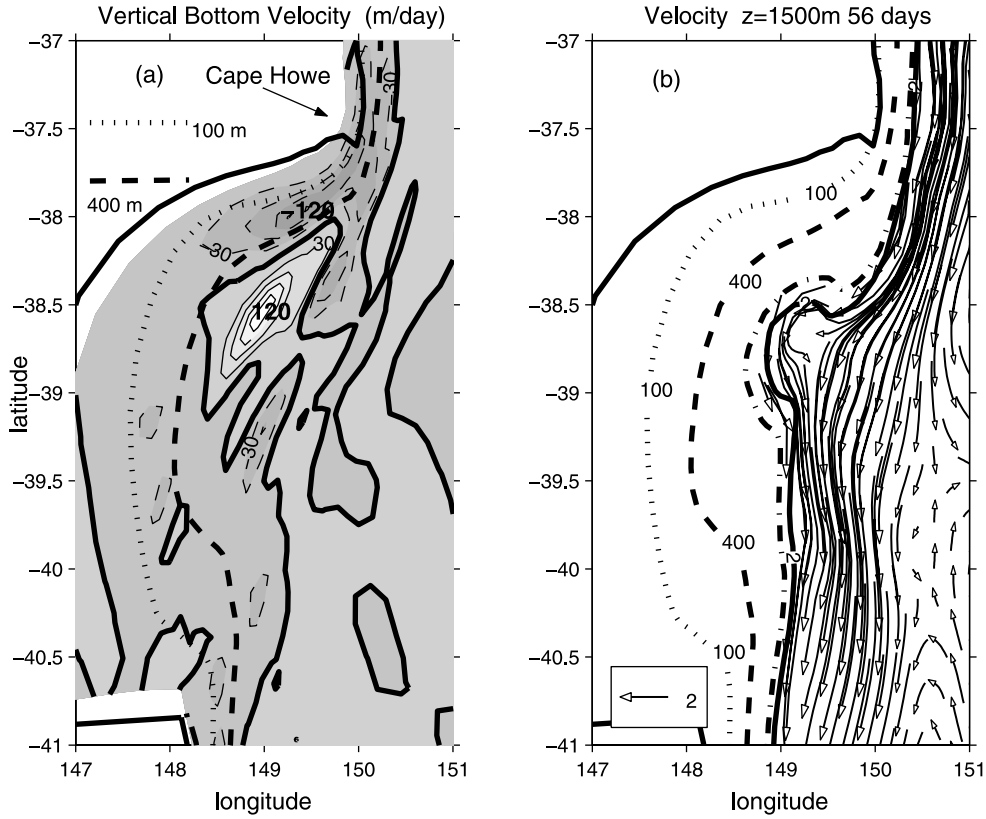

Figure 8. (a) The vertical velocity at the seafloor and at day 56 (contour interval 30 m d^{-1}). Dashed (dark shaded) contours indicate the flow is downward. The dotted and dashed curves correspond to the 100 and 400 m isobaths. (b) The horizontal velocity at day 56 and at a depth of 1500 m. A vector of length 2 cm s^{-1} is indicated. The isobaths indicated are 100 (dotted), 400 (dashed), 1500 (dash-dotted), and 2000 m (solid).

slope $h_x \sim 0.013$. The cross-slope velocity u is estimated from the quadratic law for bottom stress adopted in the model $\tau_b = C_D v^2$ through the scaling result for downwelled boundary layers

$$u_b = \tau_b / f(1 + S)H_b \quad (3)$$

[*Middleton and Ramsden*, 1996] where $C_D = 2.5 \times 10^{-3}$ is a drag coefficient, $v \sim 0.15$ cm s^{-1} a near-bottom alongshore velocity (Figure 9b), $F = -10^{-4}$ s^{-1} the Coriolis parameter and H_b the bottom boundary layer depth and taken as 20 m from Figure 9a. The parameter $S = (N h_x/f)^2$ is the Burger number and at a depth of 200 m near the slope, $N \sim 10^{-2}$ s^{-1}, so that S = 1.7. With these estimates, u is about 1 cm s^{-1} (consistent with the numerical results) and implies a vertical velocity of $w \sim -17 \times 10^{-3}$ cm s^{-1} or about 15 m d^{-1}. This scale estimate is of order that found numerically and shows that downwelling that arises from Ekman transport within the bottom boundary later is important off Cape Howe.

4. Discussion

[34] The numerical model results presented here represent years in which the EAC has strong southward extension, with a transport of 17 Sv that is 50% larger than that indicated by hydrographic data. As noted, evidence for such a strong southward penetration of the EAC comes from the study of *Luick et al.* [1994] where the observed temperature and density fields during July 1989 were similar to those obtained here: relatively warm, salty water was found off the east coast of Bass Strait. *Cresswell* [2000] also reports strong southward currents (40 cm s^{-1}) off the east coast of Tasmania.

[35] It should be noted that the 17 Sv inflow at Cape Howe and other boundary transports adopted were not "tuned" to obtain the agreement with observations found. The boundary transports were just those obtained from the OCCAM global model. Indeed, any adjustment of the EAC transport near Cape Howe would necessitate a readjustment elsewhere (to conserve mass) and this might raise more questions than it would solve.

[36] Indeed, in agreement with the observations of *Luick et al.* [1994], the model develops a front near the northeast corner of the strait and Cape Howe that separates the warm Tasman Seawater from the cold dense strait water. For this region (~38°S), both model and observations indicate the denser strait water to gravitationally cascade to depths of 300 m and as a plume that is some 5–10 km wide. The vertical velocities at a depth of 200 m can exceed 60 m d^{-1}. In accord with the observations of *Godfrey et al.* [1980], the cascade occurs below the front and the associated thermal wind shear acts to intensify the along-isobath currents with depth, to values of 20 cm s^{-1} in 200–250 m of water. Close

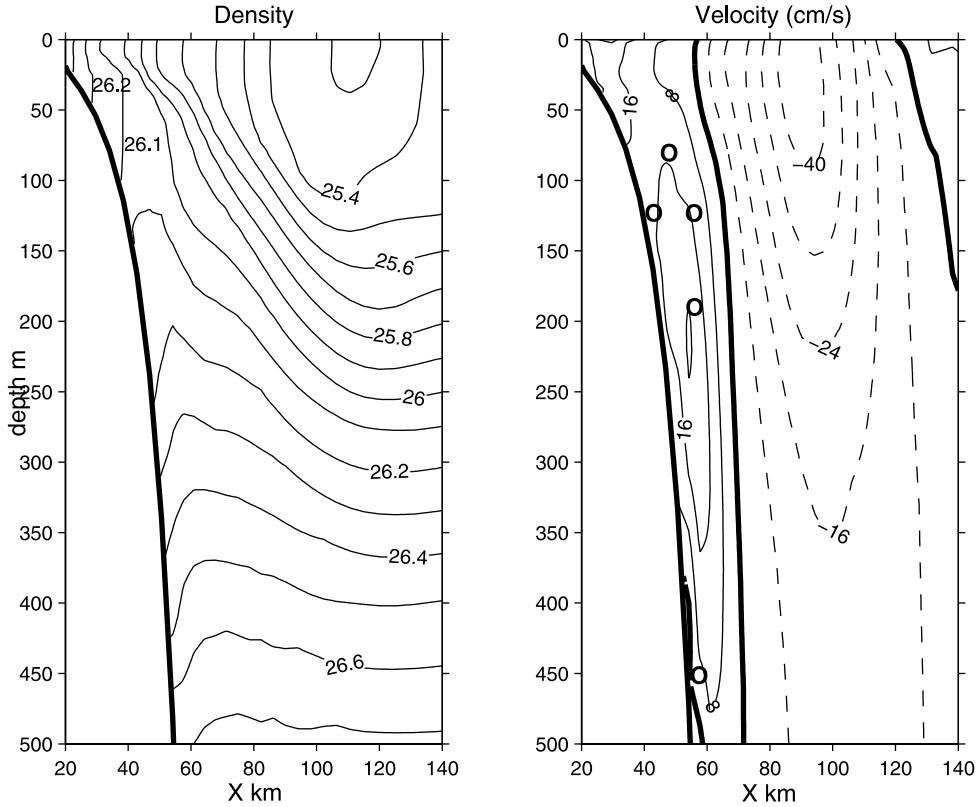

Figure 9. Results for the zonal transect 3 (J = 168) off Cape Howe (37.5°S). (a) The model density field at day 56 (interval 0.1 kg $m^{-3)}$. (b) The along-isobath velocities (contour interval 8 cm s^{-1}). Solid contours indicate flow to the north. The circles denote the locations of current meters (Table 1).

to the coast, and within Bass Strait, the model currents are of order 20–30 cm s^{-1} and also in general agreement with observations.

[37] Similar results are found off Cape Howe although the model northward currents are stronger (~15 cm s^{-1}) than indicated by the current meter data. At depths of 200 m, these strong currents lead to an Ekman transport and downwelled bottom boundary layer with vertical speeds that are also significant (~15 m d^{-1}). These deep equatorward currents arise from the thermal wind shear associated with upwelled isopycnals the EAC (Figure 9).

[38] The model also reproduces observed aspects of the hydrography and circulation off Tasmania. Off the southern tip of Tasmania, both the model and observed density fields have a 400 m deep surface mixed layer, coastal downwelling to 400 m depth and upwelling between 1500 m and 400 m: the latter a signature of the Tasman Outflow. The model indicates the Zeehan current here to extend to depths of 500 m with a transport of 1 Sv. This current is found on the east Tasmanian coast (Maria Island) and the magnitude is in accord with the ADCP results of *Cresswell* [2000] but somewhat larger than the results inferred from several moorings. Notably, the model does reproduce the circulation pattern inferred by *Cresswell* [2000] from drifter data whereby between latitudes 43° and 41.5°S, water is swept off the shelf and to the south by the EAC.

[39] In conclusion, the model adopted, while somewhat crude, has replicated many of the observed sub–weather band circulation features of the region and illustrates the important forcing mechanisms and physics of the region. Off Cape Howe, the upwelled isopycnals associated with the EAC and anticyclonic eddy, lead to an intensification of the (downwelling favourable) equatorward shelf-slope currents. The EAC will also affect the magnitude of the flow through Bass Strait through both geostrophic control and through the cascade. In the case of the latter, stronger southward excursions of warm Tasman seawater will act to enhance the gravitational cascade during winter. Off the east coats of Tasmania, the shelf slope circulation is determined by the relative strengths and convergence of the EAC and Zeehan Current.

[40] The above picture of the "mean" wintertime circulation will be augmented by the semidiurnal tides at the eastern mouth of Bass Strait [*Fandry*, 1983] which can exceed 50 cm s^{-1}. The time-averaged residual of these currents may be important but is unknown. Strong weather band fluctuations in current (~20 cm s^{-1} are also found within Bass Strait and drive coastal trapped waves northward of Cape Howe [*Middleton*, 1991; *Middleton and Black*, 1994]. Such waves, in conjunction with cold fronts may lead to episodic fluctuations in the cascade and associated circulation that we have described here.

[41] **Acknowledgments.** This research was supported by an Australian Research Council grant A39700800. M Cirano was supported by a Ph.D. Scholarship from the Brazilian CnPq for part of this study. The results were obtained using the Australian National University's Fujitsu VPP300 and APAC supercomputers, and we thank them for the time made available. We thank David Griffin for his assistance and also George Mellor and Allen Blumberg for making the Princeton model available and the Australian Geological Survey Organisation and CSIRO Marine Labo-

ratories for making the topographic data, CARS data, and East Coast Tasmanian current meter data available.

References

Baines, P. G., G. Hubert, and S. Powers (1991), Fluid transport through Bass Strait, *Cont. Shelf Res.*, *11*, 269–293.

Black, K., M. Rosenberg, G. Symonds, R. Simons, C. Pattiaratchi, and P. Nielsen (1992), Measurements of wave, current, and sea level dynamics of an exposed coastal site, paper presented at 6th International Biennial Conference on the Physics of Estuaries and Coastal Seas, Cent. for Water Res., Univ. of West. Aust., Margaret River, West. Aust., Australia.

Blumberg, A. F., and G. L. Mellor (1987), A description of a three dimensional coastal circulation model, in *Three Dimensional Coastal Ocean Models*, *Coastal Estuarine Ser.*, vol. 4, edited by N. S. Heaps, pp. 1–16, AGU, Washington, D. C.

Cirano, M., and J. F. Middleton (2004), The mean wintertime circulation along Australia's southern shelves: A numerical study, *J. Phys. Oceanogr.*, *34*, 668–684.

Cresswell, G. (2000), Currents of the continental shelf and upper slope of Tasmania, *Proc. R. Soc. Tasmania*, *133*, 23–30.

da Silva, A. M., C. C. Young, and S. Levitus (1994), *Algorithms and Procedures*, vol. 1. *Atlas of Surface Marine Data 1994*, *NOAA Atlas NESDIS 6*, 84 pp., U.S. Dep. of Comm., Washington, D. C.

Fandry, C. B. (1983), Model for the three-dimensional structure of wind-driven and tidal circulation in Bass Strait, *Aust. J. Mar. Freshwater Res.*, *34*, 121–141.

Garrett, C., and B. Toulany (1982), Sea level variability due to meteorological forcing in the northeast Gulf of St Laurence, *J. Geophys. Res.*, *87*, 1968–1978.

Gill, A. E. (1982), *Atmosphere-Ocean Dynamics*, 662 pp., Elsevier, New York.

Godfrey, J. S., I. S. Jones, J. Garry, H. Maxwell, and B. D. Scott (1980), On the winter cascade from Bass Strait into the Tasman Sea, *Aust. J. Freshwater Res.*, *31*, 275–286.

Griffin, D., M. Cahill, C. Rathbone, and N. White (2002), South-East Fishery Ocean Movies, www.marine.csiro.au/~griffin/SEF/index.htm, CSIRO Hobart, Hobart, Tasmania, Australia.

Huyer, A., R. L. Smith, P. J. Stabeno, J. A. Church, and N. J. White (1988), Currents off south-eastern Australia: Results from the Australian Coastal Experiment, *Aust. J. Mar. Freshwater Res.*, *39*, 245–288.

Klink, J. M. (1996), Circulation near submarine canyons: A modeling study, *J. Geophys. Res.*, *101*, 1211–1223.

Luick, J. L., R. Kase, and M. Tomczak (1994), On the formation and spreading of the Bass Strait Cascade, *Cont. Shelf Res.*, *14*, 385–399.

Mata, M. M., M. Tomczak, S. Wijffels, and J. A. Church (2000), East Australian Current volume transports at 30°S: Estimates from the World Ocean Circulation Experiment hydrographic sections PR11/P6 and the PCM3 current array, *J. Geophys. Res.*, *105*, 28,509–28,526.

Middleton, J. F. (1991), Coastal-trapped wave scattering into and out of straits and bays, *J. Phys. Oceanogr.*, *21*, 681–694.

Middleton, J. F., and K. P. Black (1994), The low frequency circulation in and around Bass Strait: A numerical study, *Cont. Shelf Res.*, *14*, 1495–1521.

Middleton, J. F., and D. Ramsden (1996), The evolution of the bottom boundary layer on the sloping continental shelf, *J. Geophys. Res.*, *101*, 18,061–18,077.

Ridgway, K., and J. S. Godfrey (1997), Seasonal cycle of the East Australian Current, *J. Geophys. Res.*, *102*, 22,921–22,936.

Ridgway, K., J. R. Dunn, and J. L. Wilkin (2002), Ocean interpolation by four-dimensional weighted least squares–application to the waters around Australasia, *J. Atmos. Oceanic Technol.*, *19*, 1357–1375.

Rintoul, S. R., and J. L. Bullister (1999), A late winter hydrographic section from Tasmania to the Antarctic, *Deep Sea Res., Part I*, *46*, 1417–1454.

Rintoul, S. R., and S. Sokolov (2001), Baroclinic transport variability of the Antarctic Circumpolar Current south of Australia, *J. Geophys. Res.*, *106*, 2815–2832.

Thompson, R. O. R. Y. (1983), Low-pass filters to suppress inertial and tidal frequencies, *Phys. Oceanogr.*, *13*, 1077–1083.

Tomczak, M. (1985), The Bass Strait Cascade during winter, *Cont. Shelf Res.*, *4*, 255–278.

Trenberth, K. E., J. C. Olsen, and W. G. Large (1989), A global ocean wind stress climatology based on ECMWF analyses, *Tech. Rep. NCAR/TN-338+STR*, 98 pp., Natl. Cent. for Atmos. Res., Boulder, Colo.

Webb, D. (2000), Evidence for shallow zonal jets in the South Equatorial Current Region of the southwest Pacific, *J. Phys. Oceanogr.*, *30*, 706–720.

Webb, D., B. A. de Cuevas, and A. C. Coward (1998), The first main run of the OCCAM Global Ocean Model, *Tech. Rep. 34*, Southampton Oceanogr. Cent., 43 pp., Southampton, U. K.

Wijffels, S., and G. Meyers (2004), An intersection of oceanic waveguides: Variability in the Indonesian Throughflow region, *J. Phys. Oceanogr.*, *34*, 1232–1253.

M. Cirano, Centro de Pesquisa em Geofisica e Geologia, Inst. de Geociencias, Universidade Federal da Bahia—Campus Ondina, 40170-280 Salvador-BA, Brazil.

J. F. Middleton, School of Mathematics, University of New South Wales, Sydney, NSW 2052, Australia. (john.middleton@unsw.edu.au)